JPET Fast Forward. Published on April 14, 2010 as DOI: 10.1124/jpet.110.165845
JPET Fast Forward. Published on April 14, 2010 as DOI: 10.1124/jpet.110.165845
This article has not been copyedited and formatted. The final version may differ from this version.

JPET # 165845

A Novel Autotaxin Inhibitor Reduces Lysophosphatidic Acid Levels in Plasma and the Site of Inflammation

James Gierse*, Atli Thorarensen, Konstantine Beltey, Erica Bradshaw-Pierce, Luz Cortes-Burgos, Troii Hall, Amy Johnston, Michael Murphy, Olga Nemirovskiy, Shinji Ogawa, Lyle Pegg, Matthew Pelc, Michael Prinsen, Mark Schnute, Jay Wendling, Steve Wene, Robin Weinberg, Arthur Wittwer, Ben Zweifel and Jaime Masferrer

*Pfizer Inflammation Research

700 Chesterfield Parkway N.

Chesterfield, Missouri 63017

Downloaded from jpet.aspetjournals.org at ASPET Journals on April 18, 2024

Copyright 2010 by the American Society for Pharmacology and Experimental Therapeutics.

JPET Fast Forward. Published on April 14, 2010 as DOI: 10.1124/jpet.110.165845
This article has not been copyedited and formatted. The final version may differ from this version.

JPET # 165845

Running Title: Autotaxin inhibition reduces LPA in inflammation

Corresponding Author:

James Gierse

Pfizer Inflammation Research

700 Chesterfield Parkway N.

Chesterfield, Missouri 63017

James.k.gierse@pfizer.com

gierse@sbcglobal.net

636-247-6243 (work)

314-440-6032 (cell)

314-968-3734 (home)

Text Pages: 27

Tables: 3

Figures: 6

References: 20

Abstract: 231 words

Introduction: 638 words

Discussion: 1,079 words

Nonstandard Abbreviations: LPC, lysophosphatidyl choline; LPA, lysophosphatidic acid;

FS-3, fluorescent substrate 3;

Recommended Section: Inflammation, Immunopharmacology and Asthma

Downloaded from jpet.aspetjournals.org at ASPET Journals on April 18, 2024

JPET Fast Forward. Published on April 14, 2010 as DOI: 10.1124/jpet.110.165845
This article has not been copyedited and formatted. The final version may differ from this version.

Abstract

Autotaxin is the enzyme responsible for the production of lysophosphatidic acid (LPA) from lysophosphatidyl choline (LPC) and is upregulated in many inflammatory conditions, including but not limited to cancer, arthritis and multiple sclerosis. LPA signaling causes angiogenesis, mitosis, cell proliferation and cytokine secretion. Inhibition of autotaxin may have anti-inflammatory properties in a variety of diseases, however, this hypothesis has not been tested pharmacologically due to the lack of potent inhibitors. Here we report the development of a potent autotaxin inhibitor (PF-8380) with an IC_{50} of 2.8 nM in isolated enzyme assay and 101 nM in human whole blood. PF-8380 has adequate oral bioavailability and exposures required for *in vivo* testing of autotaxin inhibition. Autotaxin's role to produce LPA in plasma and at the site of inflammation was tested in a rat air pouch model. The specific inhibitor PF-8380, dosed orally at 30 mg/kg, provided > 95% reduction in both plasma and air pouch LPA within 3 hours, indicating autotaxin is a major source of LPA during inflammation. 30 mg/kg PF-8380 reduced inflammatory hyperalgesia with the same efficacy as 30 mg/kg naproxen. Inhibition of plasma autotaxin activity correlated with inhibition of autotaxin at the site of inflammation and in *ex vivo* whole blood. Furthermore a close PK/PD relationship was observed, which suggests that LPA is rapidly formed and degraded in vivo. PF-8380 can serve as a tool compound to elucidate LPA's role in inflammation.

Downloaded from jpet.aspetjournals.org at ASPET Journals on April 18, 2024

JPET Fast Forward. Published on April 14, 2010 as DOI: 10.1124/jpet.110.165845
This article has not been copyedited and formatted. The final version may differ from this version.

Introduction

Autotaxin was first described as a mitogenic factor expressed by a variety of tumor cells and causes mitosis and angiogenesis when added to cancer cells (Stracke, Krutzsch et al. 1992). It was later determined that autotaxin's mitogenic activity resulted from its lysophospholipase D activity, converting lysophosphatidyl choline (LPC) to lysophosphatidic acid (LPA) (Umezu-Goto, Kishi et al. 2002). LPA acts through activation of five G-protein coupled receptors, referred to as LPA1-5 (Ishii, Fukushima et al. 2004), mediating changes in cell survival, proliferation and migration, tumor cell invasion, lymphocyte infiltration, angiogenesis and cytokine secretion. (Zhao, Fernandes et al. 2008). Both autotaxin and LPA receptors have been found to be upregulated in many tumor cell lines (Kishi, Okudaira et al. 2006) and that LPA induces colony scattering (prerequisite for invasion) in several tumor cells (Shin, Kim et al. 2009). Recently it has been demonstrated that a pan LPA receptor antagonist reduces the size of MDA-MB-231 tumors adapted in rats (Prestwich, Gajewiak et al. 2008)

The autotaxin LPA axis has been shown to be upregulated in variety of inflammatory conditions. In human rheumatoid arthritis (RA) the autotaxin gene is upregulated in fibroblasts from RA patients (Kehlen, Lauterbach et al. 2001) and autotaxin protein has been found in synovial fluid of patients (Nochi, Tomura et al. 2008). LPA receptor 1 is upregulated in synovial fibroblasts from RA patients (Nochi, Tomura et al. 2008). Autotaxin is one of four proteins upregulated in multiple sclerosis patients as

Downloaded from jpet.aspetjournals.org at ASPET Journals on April 18, 2024

JPET Fast Forward. Published on April 14, 2010 as DOI: 10.1124/jpet.110.165845
This article has not been copyedited and formatted. The final version may differ from this version.

demonstrated by 2-D gels (Hammack, Fung et al. 2004). LPA1 knockout mice have been shown to be resistant to neuropathic pain produced in a spinal nerve ligation model in mice (Inoue, Rashid et al. 2004). It has been hypothesized that LPA acts to produce pain by down regulating the mammalian K(2P)2.1 (KCNK2, TREK-1) channel (Cohen, Sagron et al. 2009) and Abeta-fiber-mediated spinal transmission, which underlies neuropathic pain (Xie, Matsumoto et al. 2008).

Autotaxin is found in three main isoforms, each with a different splice variant. The most stable and common β isoform is a 95 kD protein secreted by inflammatory cells and responsible for production of LPA by the hydrolysis of LPC (produced thru sPLA2) (Giganti, Rodriguez et al. 2008).

Autotaxin has been shown to be responsible for production of LPA in plasma. Autotaxin heterozygote knockout mice have a 50% reduction of circulating LPA as compared to wild-type (van Meeteren, Ruurs et al. 2006). Early autotaxin inhibitors have shown that plasma LPA, generated from endogenous LPC by incubating whole blood for several hours, can be nearly 100% inhibited, suggesting that autotaxin is the primary enzyme responsible for LPA production (Ferry, Moulharat et al. 2008). These inhibitors however were not suitable for *in vivo* use having limited solubility and bioavailability. One critical question remains, does inhibition of autotaxin reduce LPA levels at the site of inflammation? And if so, what are the consequences of that inhibition?

Downloaded from jpet.aspetjournals.org at ASPET Journals on April 18, 2024

JPET Fast Forward. Published on April 14, 2010 as DOI: 10.1124/jpet.110.165845
This article has not been copyedited and formatted. The final version may differ from this version.

To date, there have not been autotaxin inhibitors developed which regulate LPA levels *in vivo*; however, there have been several reports of inhibitors that modulate autotaxin *in vitro* or in whole blood. Inhibitors that have been described are based on substrate analogues (Prestwich, Gajewiak et al. 2008). These compounds are weak autotaxin inhibitors and are also LPA1 receptor agonist/antagonist. Recently, S32826 has been described as a potent inhibitor of autotaxin *in vitro* and in whole blood, but it's neither bioavailable nor useful for *in vivo* work (Ferry, Moulharat et al. 2008).

In this paper we describe the development of an autotaxin inhibitor that modulates LPA levels *in vitro* and *in vivo* through direct inhibition of autotaxin. The compound is capable of blocking inflammation-induced LPA synthesis, both in plasma and at the site of inflammation. This will allow further testing of the hypothesis that disruption of the autotaxin/LPA axis will have beneficial anti-inflammatory effects that could impact an array of diseases such as RA, pain and cancer.

Downloaded from jpet.aspetjournals.org at ASPET Journals on April 18, 2024

JPET Fast Forward. Published on April 14, 2010 as DOI: 10.1124/jpet.110.165845
This article has not been copyedited and formatted. The final version may differ from this version.

Methods

Materials. LPC and LPA were obtained from Avanti Polar Lipids (Birmingham, AL); all standard buffer reagents and solvents were obtained from Sigma, Chemical Co. (St. Louis, MO).

Synthesis of PF-8380

tert-butyl 4-(3-oxo-3-(2-oxo-2,3-dihydrobenzo[d]oxazol-6-yl)propyl)piperazine-1-carboxylate. 6-(3-chloropropanoyl)benzo[d]oxazol-2(3H)-one (20.0 g, 88.64 mmol) and tert-butyl piperazine-1-carboxylate (18.2 g, 97.50 mmol) was dissolved in dichloromethane (200 ml) and triethylamine (37.1 m, 266.0 mmol) added. The reaction was stirred at room temp (RT) overnight at which time it was quenched with water (100 ml) and the organics extracted with dichloromethane 2 x 50 ml. The organics were concentrated and redissolved in a small amount of diethyl ether. The flask was cooled to 0^{o}C which precipitated pure tert-butyl 4-(3-oxo-3-(2-oxo-2,3-dihydrobenzo[d]oxazol-6-yl)propyl)piperazine-1-carboxylate as a white solid (27.18 g, 72.48 mmol, 81%)

6-(3-(piperazin-1-yl)propanoyl)benzo[d]oxazol-2(3H)-one. tert-butyl 4-(3-oxo-3-(2-oxo-2,3-dihydrobenzo[d]oxazol-6-yl)propyl)piperazine-1-carboxylate (27.13 g, 72.26 mmol) was dissolved in dioxane (50 ml) and 4N HCl in dioxane (18.1 ml) added. The heterogeneous solution was stirred for 1 hour at which time the precipitate was filtered to

Downloaded from jpet.aspetjournals.org at ASPET Journals on April 18, 2024

JPET Fast Forward. Published on April 14, 2010 as DOI: 10.1124/jpet.110.165845
This article has not been copyedited and formatted. The final version may differ from this version.

give 6-(3-(piperazin-1-yl)propanoyl)benzo[d]oxazol-2(3H)-one as an off white solid. (19.87 g. 100%)

PF-8380. 6-(3-(piperazin-1-yl)propanoyl)benzo[d]oxazol-2(3H)-one (19.87 g, 72.26 mmol) was dissolved in dioxane (50 ml) and water (50 ml) to which sodium bicarbonate (16.1 g, 152 mL) was added. The solution was cooled to 0 ^{o}C and 4-nitrochloroformate (19.1 g, 94.4 mmol) added dropwise. The solution was slowly warmed to r.t. overnight. The solution was then quenched with water (300 mL) and the resulting precipitate filtered. In a separate flask (3,5-dichlorophenyl)methanol (13.0 g, 73.20 mmol was dissolved in DMF (50 ml) and sodium hydride (3.96 g, 99.0 mmol) added. The solution was stirred for 10 minutes and cooled to 0 ^{o}C. The nitro-precipitate was dissolved in DMF (50 ml) and then added dropwise to the (3,5-dichlorophenyl)methanol solution. The solution was stirred for 10 minutes and then quenched with a small amount of water to ensure quenching of excess sodium hydride. The DMF was distilled off to give a bright yellow oil which was purified by flash chromatography (5% MeOH/DCM) to give PF-8380 an off white solid (14.56 g, 30.65 mmol 42%) 1H NMR (400 MHz, DMSO-d6) d ppm 7.83 - 7.89 (2 H, m), 7.57 (1 H, s), 7.42 (2 H, s), 7.18 (1 H, d, J=7.9 Hz), 5.07 (2 H, s), 3.37 (3 H, br. s.), 3.19 (2 H, t, J=7.1 Hz), 2.89 (1 H, s), 2.73 (1 H, s), 2.70 (2 H, t, J=7.1 Hz), 2.42 (4 H, t, J=4.7 Hz) C13 NMR (400 MHz, DMSO-d6) 197.35, 154.71, 153.98, 143.37, 141.20, 135.30, 134.03, 130.81, 127.36, 126.08, 124.97, 109.33, 108.77, 64.64, 52.83, 52.25, 43.47, 35.38 M/Z = 478.1

Downloaded from jpet.aspetjournals.org at ASPET Journals on April 18, 2024

JPET Fast Forward. Published on April 14, 2010 as DOI: 10.1124/jpet.110.165845
This article has not been copyedited and formatted. The final version may differ from this version.

Murine autotaxin cloning. The full length murine autotaxin cDNA was purchased from Open Biosystems (Huntsville, AL). The following primers purchased from Integrated DNA Technologies (Coralville, IA) were used to introduce cloning sites HindIII and NotI by PCR to allow cloning into pcDNA3.1 Zeo: 5'-AGC TAG CTA AGC TTA TGG CAA GAC AAG GCT GTT TC-3' and 5'-ATG ACT GAC TGC GGC CGC TCA TTA GTG ATG ATG GTG GTG ATG AAT CTC GCT CTC ATA TGT ATG CAG G -3'. The 3' primer introduced the addition of 6-His tag to the C-terminus of the protein. The murine autotaxin gene was amplified using Accuprime Pfx DNA polymerase (Invitrogen, Carlsbad, CA). The DNA sequence of the final construct was confirmed by sequencing performed at Cogenics (Houston, TX).

Autotaxin expression. Ten liter batches of human and murine autotaxin conditioned media were prepared using a HEK293 Freestyle™ (Invitrogen, Inc.) and Wave (GE Healthcare) bioreactor transient expression system. Approximately 2.5E9 HEK cells were seeded into a Wave Bioreactor CellBag™20 containing 5 L of 293Freestyle™ media. The bag was maintained at 37˚C, 8% CO2, and a constant rocking of 25.5 rpm. When the cell density reached 2 X 10^7/ml, 4.5 L of fresh 293Freestlye™ media was added. The cells were transfected by the sterile addition of 640 ml of Opti-MEM® (Invitrogen, Inc.) containing 10 mg of plasmid DNA and 13 ml of 293Fectin™. The bioreactor was maintained under the initial growth conditions for another 6 days post transfection and the media was harvested for purification.

Downloaded from jpet.aspetjournals.org at ASPET Journals on April 18, 2024

JPET Fast Forward. Published on April 14, 2010 as DOI: 10.1124/jpet.110.165845
This article has not been copyedited and formatted. The final version may differ from this version.

Autotaxin purification. Concentrated HEK cell media was buffered to pH 8.0 with Trizma pre-set crystals and octyl-beta-D-pyranoside added to 0.05% with 300 mM NaCl. Protein was initially captured using Ni-NTA Superflow resin and further purified using Q-Sepharose FF resin. Samples containing autotaxin with a purity greater than 80% (as determined by SDS-PAGE) were pooled, concentrated and further purified using a Superdex 200 (16/60) column run in 50 mM Tris, pH 8.0, 150 mM NaCl and 0.05% octyl-beta-D-pyranoside. Fractions containing autotaxin with purity greater than 95% were pooled concentrated and stored at -80^{o}C.

Recombinant enzyme assay. FS-3 substrate (Echelon L-2000) was solubilized in assay buffer at 500 μM and frozen at -20˚C in single use aliquots for up to 4 weeks. Recombinant autotaxin was diluted in Tris buffered saline (140 mM NaCl, 5 mM KCl, 1 mM $CaCl_2$, 1 mM $MgCl_2$, 50 mM Tris, pH 8.0) and incubated with compound in DMSO or DMSO alone (final 1% DMSO) for 15 minutes at 37˚C and the reaction started with the addition of FS-3 at a final concentration of 1 μM. The reaction was allowed to proceed at 37˚C for 30 minutes and monitored at 520 nm until the uninhibited control when compared to a no enzyme control gave a Z' ≥0.5. IC50's were determined in triplicate using a 4 parameter fit.

Recombinant enzyme assay using LPC LC-MS/MS. 17:0 LPC and 16:0 LPA were dissolved in MeOH (10 mg/ml and100 mg/ml respectively) and maintained at -20˚C. Recombinant autotaxin was diluted in Dulbecco's Modified Eagle's Medium (DMEM) and added to compound in DMSO or DMSO alone (final 1% DMSO) and the reaction

Downloaded from jpet.aspetjournals.org at ASPET Journals on April 18, 2024

JPET Fast Forward. Published on April 14, 2010 as DOI: 10.1124/jpet.110.165845
This article has not been copyedited and formatted. The final version may differ from this version.

started with the addition of LPC at a final concentration of 15 μγ/ml followed by incubation at 37˚C for 30 minutes. The reaction was stopped by the addition of 2 volumes of organic (50:50:1;ACN:Methanol:Acetic Acid + 15 ng/ml C16:0 LPA, IS) and either frozen at -80˚C or diluted further in preparation for LC-MS/MS. Autotaxin LPC assay was diluted 3:7 with 66% Methanol/water plus 0.1% TEA and analyzed by LC-MS/MS.

Fetal fibroblast cell assay. Human fetal fibroblast were prepared from foreskin and cultured as described (Hawley, Sullivan et al. 1980; Raz, Wyche et al. 1989). Cells were grown in DMEM containing 10% fetal bovine serum (FBS), 4 mM L-Glutamine, 25 mM HEPES, 100 U/ml penicillin and 100 μg/ml streptomycin (Invitrogen, Carlsbad, CA) and were passed when confluent. The cells were suspended in FBS-free DMEM and plated at density of 5 x 10^4 cells/well on 96-well culture plate (Corning, NY). After 24 hours of incubation, various concentrations of compound were added with Tyrosine protein phosphatase inhibitor cocktail (Millipore, Temecula, CA, USA). After 15 minutes incubation, the substrate C17:0 LPC (final 15 μg/ml) was added to start the autotaxin enzyme reaction. After 30 minutes at 37 º C, the supernatant of cell culture was collected and mixed with organic solution, acetonitrile:methanol:acetic acid (50:50:1, v/v/v)(EMD chemicals, Gibbstown, NJ), to stop the reaction. C17:0 LPA content was measured by LC-MS/MS.

Autotaxin inhibition in human whole blood. Venous blood from healthy human donors was collected in heparinized tubes. Blood (0.5 ml) was incubated with compound

Downloaded from jpet.aspetjournals.org at ASPET Journals on April 18, 2024

JPET Fast Forward. Published on April 14, 2010 as DOI: 10.1124/jpet.110.165845
This article has not been copyedited and formatted. The final version may differ from this version.

dissolved in DMSO (1% final concentration of DMSO) in 96-well collection plates for 2 hours at 37^{o}C. The reaction was stopped by centrifugation at 800 x g for 10 minutes to pellet the cells. Plasma supernatant (100 ul) was precipitated with 3 volumes of methanol/acetonitrile/Acetic acid (60:40:1) and spun at 4,000 x g for 10 minutes. Supernatants were recovered and diluted. LPA was measured by LC-MS/MS. Ten concentrations of compound starting at 10 μM with 3 fold dilutions were examined in duplicate. IC_{50} values were generated by fitting the data with a four parameter logistic regression fit then determining the point that intersects 50% of the difference between negative (time zero) and positive (2 hours) uninhibited controls (control IC_{50}).

LPA mass spectrometry. Panels of LPA species including C16:0, C18:0, C18:1 and C20:4 were analyzed using an LC-MS/MS method modified from the published method by Chen et al (Chen, Kuo et al. 2008) Briefly, 50 μl of sample was extracted with 350 μl of acetonitrile:methanol:acetic acid (50:50:1) containing a C17:0 LPA at 5 ng/ml as internal standard. 300-μL of supernatant was removed and 700 μl of methanol:water:triethylamine (TEA) (66:34:0.1) was added prior to analysis. Quantitation experiments were performed by 2D LC-MS/MS utilizing an HP 1200 LC system (Agilent, Palo Alto, CA) composed of a quaternary pump, a CTC Analytics HTS PAL autosampler (LEAP Technologies, Carrboro, NC), and a switching valve, plumbed in-line with HP 1100 HPLC pump which was interfaced to an API 4000 Qtrap mass spectrometer (MDS-Sciex, Toronto, Canada) operated in the negative ion electrospray and multiple-reaction-monitoring (MRM) modes. Typically, 300 μL of sample was injected onto a Betasil C18 column (Thermo Scientific, Waltham, MA) with 1 ml/min 25

Downloaded from jpet.aspetjournals.org at ASPET Journals on April 18, 2024

JPET Fast Forward. Published on April 14, 2010 as DOI: 10.1124/jpet.110.165845
This article has not been copyedited and formatted. The final version may differ from this version.

mM ammonium acetate:methanol 50:50 mixture. After 3 minutes, the valve was switched and the captured analytes were eluted onto a 3.0 x 50 mm, 3.5 μm particle size XBridge C8 analytical column (Waters, Beverly, MA) with a 3 minute gradient at 0.8 ml/min flow rate. Gradient mobile phases were A) methanol:methylene chloride:water (55:5:40) with 0.1% TEA and B) methanol:methylene chloride (50:50) with 0.1% TEA.

Selected analytes were specifically detected by monitoring HPLC retention times and ion pairs corresponding to the parent and specific fragment ion mass-to-charge ratios.

Rat pharmacokinetics. Male Lewis rats weighing 275 to 300 grams were purchased from Charles River Laboratories (Wilmington, DE) and acclimated to their surroundings for approximately one week with food and water provided ad libitum. A minimum of one day prior to study, animals were anesthetized with Isoflurane (to effect) and implanted with Culex (BASi, West Lafayette, IN) vascular catheters in the carotid artery. Animals were acclimated in Culex cages overnight prior to dosing. Patency of the carotid artery catheter was maintained using the "tend" function of Culex ABS. Animals were dosed with PF-8380 at 1, 3, 10, 30 and 100 mg/kg by oral gavage following an overnight fast. Blood collections were obtained from the carotid artery and performed by the Culex at 0.25, 0.5, 1, 2, 4, 6, 8 and 24 hours post administration. Blood was centrifuged and plasma collected for analysis of PF-8380 and LPA concentrations.

Downloaded from jpet.aspetjournals.org at ASPET Journals on April 18, 2024

JPET Fast Forward. Published on April 14, 2010 as DOI: 10.1124/jpet.110.165845
This article has not been copyedited and formatted. The final version may differ from this version.

Pharmacodynamic modeling. The LPA data obtained during the rat pharmacokinetic study was fit to the inhibitory E_{max} pharmacodynamic model described by the following equation:

$$E = E_{\max} - \left(E_{\max} - E_0\right) \times \left(\frac{C_p}{C_p + EC_{50}} \right) \qquad \text{Eq. 1}$$

where the effect (E) is E_{max} at a plasma concentration of zero ($C_p = 0$) and E_0 as the plasma concentration approaches infinity ($C_p = \infty$). EC_{50} represents the concentration required to achieve 50% of the maximal inhibitory effect. Pharmacodynamic modeling was conducted using all plasma concentration and respective LPA concentration data with WinNonlin version 5.2 (Pharsight, Mountain View, CA).

Sample Preparation and LC-MS/MS Analysis of Plasma for PF-8380. 50 µL of plasma were mixed with 150 µL acetonitrile containing LPA 17:0 internal standard and centrifuged to pellet precipitated proteins. Supernatant from each sample was analyzed on a Sciex API4000 LC-MS/MS system equipped with 2 Shimadzu LC-10AD VP binary pumps and Leap HTC PAL autosampler. A five µl sample extract was injected onto a Thermo Aquasil C18 (2.1 x 30mm, 3 µm) analytical column and eluted using a linear gradient with mobile phase consisting of 0.1% formic acid and 0.1% formic acid in acetonitrile. PF-8380 was analyzed using Turbo IonSpray in ESI+ mode with multiple reaction monitoring of parent/daughter ions at m/z 478.1/161.0.

Carrageenan-induced LPA in the rat air pouch. Male Lewis rats 175 - 200 g, (Charles River Laboratories, Wilmington, MA) were used in the study. Air pouches were

Downloaded from jpet.aspetjournals.org at ASPET Journals on April 18, 2024

JPET Fast Forward. Published on April 14, 2010 as DOI: 10.1124/jpet.110.165845
This article has not been copyedited and formatted. The final version may differ from this version.

produced by subcutaneous injection of 20 ml of sterile air into the intrascapular area of the back. Pouches were allowed to develop for 1 day. Animals (6 per group) were fasted with free access to water for 16 to 24 hours prior to drug administration. Drug, vehicle or 1 mg/kg dexamethazone (Dex) were administered by oral gavage 1 hour prior to injection of 2 ml of a 1% suspension of carrageenan (FMC BioPolyer, Philadelphia PA) dissolved in saline into the pouch. At 3 hours post-carrageenan injection, the pouch fluid was collected by lavage with 2 ml of PBS containing 10 μM sodium fluoride (Sigma Chemical, St. Louis MO). The fluid was centrifuged at 800g for 10 minutes at 4^{o}C and the supernatants were collected for LPA analysis by LC-MS/MS. Blood samples were collected into 10 ml heparinized tubes (Vacutainer tubes; Becton Dickenson, Franklin Lakes NJ) 4 h post dosing and immediately centrifuged at 800g for 10 minutes at 4^{o}C and then frozen at -80 ^{o}C. For analysis of autotoxin activity, samples of both pouch and plasma were incubated at room temperature for 4 hours. LPA was produced from existing LPC and autotoxin levels in those fluids. The difference in LPA levels from time 0 to 4 hours was used to calculate autotoxin activity.

Rat adjuvant induced arthritis hyperalgesia. Inflammation was established in female Lewis rats (150-200 g, Harlan, Indianapolis, IN). Five animals per dose group were injected with 3 mg/kg; heat killed Mycobacterium Butyricum suspended in paraffin oil subcutaneously on the base of the tail (Day 0). By Day 10-14 rats manifest signs of disease and vocalization baselines were taken by flexing the right and left knees each 10 times. Rats that vocalized at least 5 times/hindlegs were included in the study. Animals were treated orally bid with 10, 30 or 100 mg/kg PF-8380, or 30 mg/kg naproxen

Downloaded from jpet.aspetjournals.org at ASPET Journals on April 18, 2024

JPET Fast Forward. Published on April 14, 2010 as DOI: 10.1124/jpet.110.165845
This article has not been copyedited and formatted. The final version may differ from this version.

(positive control), or vehicle and vocalization was assessed on day 3, 2 hours post administration.

Downloaded from jpet.aspetjournals.org at ASPET Journals on April 18, 2024

JPET Fast Forward. Published on April 14, 2010 as DOI: 10.1124/jpet.110.165845
This article has not been copyedited and formatted. The final version may differ from this version.

Results

PF- 8380. Screening of our compound collection identified numerous leads for our medicinal chemistry program. Our medicinal chemistry effort rapidly optimized the lead matter by improving potency and pharmacokinetics properties resulting in the identification of PF-8380 (Figure 1) as a suitable tool compound for *in vivo* evaluation.

***In vitro* potency.** Potency of PF-8380 was confirmed as low nM utilizing several assay methods. Each method differed by substrate and sources/species of enzyme. The data are summarized in Table 1. Recombinant human enzyme (β isoform), purified from HEK293 cells was utilized with the high throughput screening assay of the fluorescent substrate FS-3 and LPC 17:0 as substrates. Both substrates were run at similar enzyme concentrations (approximately 5 nM) and incubation and reaction times. Both substrates gave similar low nM IC_{50}'s. PF-8380 also inhibited rat autotaxin with an IC_{50} of 1.16 nM with FS-3 substrate. Potency of PF-8380 was maintained when utilizing enzyme produced from fetal fibroblasts used in combination with LPC as a substrate. In human whole blood incubated with compound for 2 hours, autotaxin was inhibited with an IC_{50} of 101 nM.

Pharmacokinetics. The pharmacokinetic profile of PF -8380 was evaluated at an IV dose of 1 mg/kg and oral doses of 1 to 100 mg/kg out to 24 hours (Figure 2A & B). PF-8380 has mean clearance of 31 mL/min/kg, volume of distribution at steady state of 3.2 L/kg, and effective $t_{1/2}$ of 1.2 hours (Table 2). Oral bioavailability is moderate ranging

Downloaded from jpet.aspetjournals.org at ASPET Journals on April 18, 2024

JPET Fast Forward. Published on April 14, 2010 as DOI: 10.1124/jpet.110.165845
This article has not been copyedited and formatted. The final version may differ from this version.

from 43 to 83% (Table 2). Plasma concentrations increase with single oral escalating doses (Figure 2B) but Cmax increases at a rate that is approximately proportional to dose from 1 to 10 mg/kg and less than proportional to dose from 10 to 100 mg/kg (Figure 2C). PF-8380 exposures estimated by area under the curve are approximately proportional to dose and linear up to 100 mg/kg (Figure 2C). Plasma C16:0, C18:0 and C20:0 LPA levels were measured immediately following collection (Figure 2D shows C18:0 LPA levels at all doses). Maximal reduction of LPA levels were observed by the 3 mg/kg dose at 0.5 hours with all LPA returning at or above baseline at 24 hours.

PF-8380 Pharmacodynamics. The pharmacodynamic effect of PF-8380 was measured as decreasing C16:0, C18:0 and C20:0 LPA levels in the plasma. The plasma LPA levels and PF-8380 concentrations were fit to an inhibitory E_{max} model and the model parameters (EC_{50}, E_{max}, and E_0) for each LPA are presented in Table 3. The effect of PF-8380 on plasma LPA levels indicates a direct response (Supplementary data Figure 1-4). Data show that LPA concentrations decline rapidly and reaches it's maximal inhibition between 15 and 30 minutes post administration for all doses levels, corresponding with PF-8380 plasma t_{max} (Table 2). It is interesting to note that the EC_{50} values obtained (means = 51.7 – 84.6 nM) are similar to the IC_{50} value obtained from human whole blood in the *in vitro* potency assay (Table 1).

***In vivo* modulation of LPA levels.** Reduction of LPA *in vivo,* both in plasma and at the site of inflammation was evaluated in a rat air pouch model of inflammation. PF-8380 was dosed orally and provided dose proportional blood levels from 0.079 at 3 mg/kg to

Downloaded from jpet.aspetjournals.org at ASPET Journals on April 18, 2024

JPET Fast Forward. Published on April 14, 2010 as DOI: 10.1124/jpet.110.165845
This article has not been copyedited and formatted. The final version may differ from this version.

2.68 μM at 100 mg/kg at 4 hours post dose. LPA was evaluated from plasma and pouch fluid immediately after collection and after a 4 hour incubation (Figure 3). Autotaxin activity was calculated as a formation rate of LPA (Figure 4). Autotaxin was inhibited up to 95% in both plasma and air pouch at 100 mg/kg. Dose responsive inhibition of autotaxin activity in plasma and pouch was correlated with human whole blood (Figure 5). EC60 is approximately 0.08 μM for inhibition in human whole blood, in vivo rat plasma and rat air pouch and EC90 is approximately 2 μM for all three (human whole blood, plasma and pouch).

Inhibition of inflammatory hyperalgesia. Utilizing vocalization as a measure of inflammatory hyperalgesia, PF-8380 reduced hyperalgesia in a dose responsive manner with the same efficacy as 30 mg/kg naproxen (figure 6). PF-8380 had maximal efficacy at 30 mg/kg as compared to 30 mg/kg naproxen. This dose corresponds to maximal inhibition of LPA levels both in plasma and the site of inflammation.

Downloaded from jpet.aspetjournals.org at ASPET Journals on April 18, 2024

JPET Fast Forward. Published on April 14, 2010 as DOI: 10.1124/jpet.110.165845
This article has not been copyedited and formatted. The final version may differ from this version.

Discussion

A high throughput screening assay for autotaxin inhibitors using FS-3 produced many potent chemical series. A handful of inhibitors of ATX have appeared in the literature (Parrill and Baker 2008). A recent report claimed a series of ATX inhibitors inspiring us to engage in SAR aimed at identifying a suitable tool compound (Schiemann et al, 2009). Our medicinal chemistry effort rapidly explored the SAR in this lead series with a focus on improved potency and pharmacokinetics properties resulting in the identification of PF-8380 as a suitable tool compound for *in vivo* evaluation

When these were tested further either using LPC as a substrate or utilizing enzyme produced from a cell line, many series were much less potent. The series, which included PF-8380, maintained their potency both when using LPC of FS-3 as a substrate and using either recombinant or enzyme secreted by fetal fibroblast cells. Subsequent analogues synthesized within this series produced PF-8380, with nM potency in enzyme assays and 100 nM potency in human whole blood. Several observations suggest that PF-8380 is a tight-binding inhibitor of autotaxin with sub-nanomolar potency. PF-8380 appears to be competitive with substrate (data not shown). Traditional kinetic analysis was complicated by apparent substrate inhibition in the FS-3 substrate assay with a K_m of about 3 µM and a K_i for substrate inhibition of the enzyme-substrate complex of about 13 µM. However, IC_{50}'s of PF-8380 determined at 1, 5, 10 and 20 µM substrate showed little effect of substrate escalation on the IC50. Rather than the 6-fold increase in IC_{50} between 1 and 20 uM expected for a competitive inhibitor, an increase of only 1.2-fold was observed. This suggests that the K_i for PF-8380 is much smaller than the enzyme

Downloaded from jpet.aspetjournals.org at ASPET Journals on April 18, 2024

JPET Fast Forward. Published on April 14, 2010 as DOI: 10.1124/jpet.110.165845
This article has not been copyedited and formatted. The final version may differ from this version.

concentration in the assay (2-5 nM). In fact, the slope and intercept of a plot of IC_{50} versus substrate concentration were consistent with a K_i of about 0.04 nM and an enzyme concentration of 2.2 nM (data not shown). Additionally, a direct fit of enzyme activity versus inhibitor concentration data using the Morrison equation for tight-binding inhibitors yielded a Ki of 0.02 nM and an enzyme concentration of 2.6 nM (data not shown). These observations indicate that under the conditions of the recombinant enzyme assays, PF-8380 is essentially titrating the enzyme active site.

Since most preclinical animal models are done in rodents, the potency of PF-8380 was evaluated against rat autotaxin. Rat and murine autotaxin sequences are identical, so these measurements can be used for either species. The potency in the recombinant enzyme assay were comparable to human. A determination was made that human whole blood assays could be used to estimate potency in a rodent system. Human whole blood potency was shifted as expected to the right, probably due to protein binding. PF-8380 inhibited plasma autotaxin activity > 90% indicating that it is the major source of LPA production in plasma.

Analysis of a pharmacokinetic/pharmacodynamic (PK/PD) relationship was attempted by measuring plasma LPA. Our initial observations with human whole blood and the observation in autotaxin heterozygote knockout animals indicate that autotaxin is the major source of LPA in plasma. In order to determine a PK/PD effect however, the rate of biosynthesis/degredation of LPA needs to be taken into account. Whole blood assays depend on an incubation period from several up to 24 hours to produce LPA from plasma autotaxin activity. The analysis done in this paper was careful to limit the time of

Downloaded from jpet.aspetjournals.org at ASPET Journals on April 18, 2024

JPET Fast Forward. Published on April 14, 2010 as DOI: 10.1124/jpet.110.165845
This article has not been copyedited and formatted. The final version may differ from this version.

incubation of the plasma post sampling, but with many time points it was difficult to obtain samples at precisely the right time, meaning that there was most certainly some incubation time. In any event, LPA levels were rapidly reduced following oral dosing, indicating that LPA present at basal levels in the plasma is rapidly degraded.

Analysis of the *in vivo* effects of PF-8380 on production of LPA in plasma and in the inflamed air pouch indicates a close correlation between plasma, pouch and *ex vivo* whole blood inhibition of autotaxin activity. Plasma and pouch samples were collected immediately and processed for LPA analysis. Plasma samples without incubation to determine autotaxin activity did not show a dose dependent decrease in LPA as was seen in the PK study. Plasma that was incubated for 4 hours at RT showed a very good dose response. This indicated that basal LPA levels are not as sensitive to autotaxin inhibition and that analysis of autotaxin activity needs to be performed to determine a PK/PD relationship. Pouch samples on the other hand, either with 4 hours of incubation or no incubation, both showed a similar dose response. Presumably the pouch , with a robust inflammatory condition produces much more autotaxin, hence higher basal levels of LPA and is sensitive to autotaxin inhibition.

In order to estimate doses necessary to inhibit LPA formation *in vivo* at the site of inflammation, a correlation of human whole blood inhibition of plasma autotaxin activity and air pouch autotaxin activity indicate that there is a close correlation of the three. This suggests that a whole blood assay can be an accurate measure of subsequent doses needed to completely inhibit the production of LPA at the site of inflammation. Autotaxin's role

Downloaded from jpet.aspetjournals.org at ASPET Journals on April 18, 2024

JPET Fast Forward. Published on April 14, 2010 as DOI: 10.1124/jpet.110.165845
This article has not been copyedited and formatted. The final version may differ from this version.

in the production of LPA at the site of inflammation was then tested with PF-8380. Immediately after samples were taken from the pouch LPA levels were analyzed, this minimized LPA formation by autotaxin activity in the fluid. LPA levels in the pouch were inhibited >90% indicating that autotaxin is the primary source of LPA at the site of inflammation. PF-8380 was evaluated for its inhibition of inflammatory hyperalgesia in rat adjuvant induced arthritis. Maximal efficacy in hyperalgesia was equal to naproxen at 30 mg/kg. In previous studies, naproxen dosed orally at 10 mg/kg that was determined from biomarker data to be efficacious to inhibit PGE2 thus both forms of cyclooxygenase. A dose of naproxen 3 times higher was used in this study, which represents maximal effect based on cyclooxygenase. Naproxen at 100 mg/kg produces side effects in rats such as GI side effect that will not provide mechanism-based data and therefore we did not test higher doses than 30 mg/kg. This indicated that hyperalgesia caused by adjuvant induced arthritis is primarily peripheral, since the LPA biomarkers in this study were peripheral measures of LPA reduction.

In summary, this is the first report of an inhibitor of autotaxin that reduces LPA levels *in vivo*. PF-8380 has been demonstrated to be a potent inhibitor of autotaxin *in vitro* using native enzyme and substrate and also in *ex vivo* human whole blood. PF-8380 is bioavailable and can be dosed *in vivo* to levels that are several multiples above the ED80, which can be accomplished with twice a day dosing at 10 mg/kg. Autotaxin's role in the production of LPA at the site of inflammation was confirmed in the rat air pouch model of inflammation. Autotaxin was inhibited > 90% both in plasma and at the site of inflammation by PF-8380, indicating that autotaxin is the primary enzyme responsible for

Downloaded from jpet.aspetjournals.org at ASPET Journals on April 18, 2024

JPET Fast Forward. Published on April 14, 2010 as DOI: 10.1124/jpet.110.165845
This article has not been copyedited and formatted. The final version may differ from this version.

the production of LPA at the site of inflammation. Measurement of autotaxin activity in *ex vivo* whole blood or plasma can be used to calculate dose projections and PF-8380 can now be used as a pharmacological tool to evaluate the role that LPA plays in inflammation and cancer.

Downloaded from jpet.aspetjournals.org at ASPET Journals on April 18, 2024

JPET Fast Forward. Published on April 14, 2010 as DOI: 10.1124/jpet.110.165845
This article has not been copyedited and formatted. The final version may differ from this version.

Acknowledgements

The authors would like to acknowledge those whose contributions would not have made this paper possible: Pat Griffin of the Scripps Institute (Jupiter Florida) for the human autotaxin clone and initial high-throughput assay development; James Valentine, Karen Mattison, Mark Tibbetts and Steve Hawrylik of The Pfizer Biomolecular Screening Group for screening the Pfizer compound library for initial autotaxin hits.

Animal Use

The Pfizer Institutional Animal Care and Use Committee reviewed and approved the animal use in these studies. The animal care and use program is fully accredited by the Association for Assessment and Accreditation of Laboratory Animal Care, International.

Downloaded from jpet.aspetjournals.org at ASPET Journals on April 18, 2024

JPET Fast Forward. Published on April 14, 2010 as DOI: 10.1124/jpet.110.165845
This article has not been copyedited and formatted. The final version may differ from this version.

References

Chen, Y. Q., M. S. Kuo, et al. (2008) AGPAT6 is a novel microsomal glycerol-3-phosphate acyltransferase. *J Biol Chem* **283**(15): 10048-57.

Cohen, A., R. Sagron, et al. (2009) Pain-associated signals, acidosis and lysophosphatidic acid, modulate the neuronal K(2P)2.1 channel. *Mol Cell Neurosc i***40**(3): 382-9.

Ferry, G., N. Moulharat, et al. (2008) S32826, a nanomolar inhibitor of autotaxin: discovery, synthesis and applications as a pharmacological tool. *J Pharmacol Exp The* **327**(3): 809-19.

Giganti, A., M. Rodriguez, et al. (2008) Murine and human autotaxin alpha, beta, and gamma isoforms: gene organization, tissue distribution, and biochemical characterization. *J Biol Chem* **283**(12): 7776-89.

Hammack, B. N., K. Y. Fung, et al. (2004) Proteomic analysis of multiple sclerosis cerebrospinal fluid. *Mult Scler* **10**(3): 245-60.

Hawley, N. P., J. E. Sullivan, et al. (1980) Optimized conditions for the growth of human epidermal cells in culture. *The Journal of investigative dermatology* **75**(2): 176-82.

Downloaded from jpet.aspetjournals.org at ASPET Journals on April 18, 2024

JPET Fast Forward. Published on April 14, 2010 as DOI: 10.1124/jpet.110.165845
This article has not been copyedited and formatted. The final version may differ from this version.

Inoue, M., M. H. Rashid, et al. (2004) Initiation of neuropathic pain requires lysophosphatidic acid receptor signaling. *Nat Med* **10**(7): 712-8.

Ishii, I., N. Fukushima, et al. (2004) Lysophospholipid receptors: signaling and biology. *Annu Rev Biochem* **73**: 321-54.

Kehlen, A., R. Lauterbach, et al. (2001) IL-1 beta- and IL-4-induced down-regulation of autotaxin mRNA and PC-1 in fibroblast-like synoviocytes of patients with rheumatoid arthritis (RA). *Clin Exp Immuno l***123**(1): 147-54.

Kishi, Y., S. Okudaira, et al. (2006) Autotaxin is overexpressed in glioblastoma multiforme and contributes to cell motility of glioblastoma by converting lysophosphatidylcholine to lysophosphatidic acid. *J Biol Chem* **281**(25): 17492-500.

Nochi, H., H. Tomura, et al. (2008) Stimulatory role of lysophosphatidic acid in cyclooxygenase-2 induction by synovial fluid of patients with rheumatoid arthritis in fibroblast-like synovial cells. *J Immuno l***181**(7): 5111-9.

Parrill AL, Baker DL (2008) Autotaxin inhibition: challenges and progress toward novel anti-cancer agents. *Anti-Cancer Agent Med. Chem **Dec 8(***8): 917-923.

Downloaded from jpet.aspetjournals.org at ASPET Journals on April 18, 2024

JPET Fast Forward. Published on April 14, 2010 as DOI: 10.1124/jpet.110.165845
This article has not been copyedited and formatted. The final version may differ from this version.

Prestwich, G. D., J. Gajewiak, et al. (2008) Phosphatase-resistant analogues of lysophosphatidic acid: agonists promote healing, antagonists and autotaxin inhibitors treat cancer. *Biochim Biophys Acta* **1781**(9): 588-94.

Raz, A., A. Wyche, et al. (1989) Temporal and pharmacological division of fibroblast cyclooxygenase expression into transcriptional and translational phases. *Proceedings of the National Academy of Sciences of the United Statesof America* **86**(5): 1657-61.

Schiemann K, Schultz M, et al. (2009) Preparation of piperidines and piperazines as antitumor agents. *PCT Int. Appl*. WO2009046841

Shin, K. J., Y. L. Kim, et al. (2009) Lysophosphatidic acid signaling through LPA receptor subtype 1 induces colony scattering of gastrointestinal cancer cells. *J Cancer Res Clin Oncol* **135**(1): 45-52.

Umezu-Goto, M., Y. Kishi, et al. (2002) Autotaxin has lysophospholipase D activity leading to tumor cell growth and motility by lysophosphatidic acid production. *J Cell Biol* **158**(2): 227-33.

van Meeteren, L. A., P. Ruurs, et al. (2006) Autotaxin, a secreted lysophospholipase D, is essential for blood vessel formation during development. *Mol Cell Biol* **26**(13): 5015-22.

Downloaded from jpet.aspetjournals.org at ASPET Journals on April 18, 2024

JPET Fast Forward. Published on April 14, 2010 as DOI: 10.1124/jpet.110.165845
This article has not been copyedited and formatted. The final version may differ from this version.

Xie, W., M. Matsumoto, et al. (2008) Involvement of LPA1 receptor signaling in the reorganization of spinal input through Abeta-fibers in mice with partial sciatic nerve injury. *Mol Pain* **Oct. 15**(4): 46.

Zhao, C., M. J. Fernandes, et al. (2008) Regulation of lysophosphatidic acid receptor expression and function in human synoviocytes: implications for rheumatoid arthritis? *Mol Pharmacol* **73**(2): 587-600.

Downloaded from jpet.aspetjournals.org at ASPET Journals on April 18, 2024

JPET Fast Forward. Published on April 14, 2010 as DOI: 10.1124/jpet.110.165845
This article has not been copyedited and formatted. The final version may differ from this version.

Legends for Figures

Fig. 1 Structure of PF-8380.

Fig. 2. Pharmacokinetics of PF-8380 in rat. A) Plasma concentration-time profile following intravenous administration of 1 mg/kg PF-8380 to Wistar Rats. B) Plasma concentration-time profile following various single oral doses C) Exposures at Cmax and AUC by dose D) Plasma concentration-time profiles of LPA 18:1 levels immediately ± SEM after collection.

Fig. 3. *In vivo* inhibition of LPA generation by PF-8380. Various amounts of PF-8380, or dexamethasone (1 mg/kg) were dosed orally 1 hour prior to injection of carrageenan in rat air pouch (n=6 rats per group). 3 hours post carrageenan injection plasma and pouch fluid were collected and LPA analyzed by mass spec. Plotted are total LPA of 4 major species immediately following collection from: A) plasma and B) air pouch, then 4 hours incubation at RT. C) plasma and D) air pouch.

Fig. 4. *In vivo* inhibition of autotaxin activity by PF-8380. Autotaxin activity inhibition was measured by incubation of rat A) plasma and B) pouch fluid for 4 hours at RT. Plotted is the average total LPA measured by mass spec from 6 animals per group.

Fig. 5. Correlation of autotaxin activity inhibition in human whole blood, rat plasma and rat air pouch. Percent inhibition of autotaxin activity is plotted vs. concentration of

Downloaded from jpet.aspetjournals.org at ASPET Journals on April 18, 2024

JPET Fast Forward. Published on April 14, 2010 as DOI: 10.1124/jpet.110.165845
This article has not been copyedited and formatted. The final version may differ from this version.

PF-8380 for human whole blood, rat plasma and rat inflammatory air pouch following 4 hours post oral dosing and 3 hours post carrageenan. Autotaxin activity was determined as the rate of formation of LPA 18:1 for 4 hours at RT. Human whole blood is the average ± SEM for three donors. *In vivo* plasma and pouch is the % inhibition of an average of 6 animals per group.

Fig. 6. Inhibition of hyperalgesia associated with adjuvant induced arthritis by PF-8380.

In female Lewis rats (5 animals per dose group) were treated orally bid with 10, 30 or 100 mg/kg PF-8380, or 30 mg/kg naproxen (positive control), or vehicle and vocalization was assessed on day 3, 2 hours post administration. Plotted is average % inhibition of vehicle vs. control ± SEM.

Downloaded from jpet.aspetjournals.org at ASPET Journals on April 18, 2024

JPET Fast Forward. Published on April 14, 2010 as DOI: 10.1124/jpet.110.165845
This article has not been copyedited and formatted. The final version may differ from this version.

Tables

Table 1. *In vitro* Potency of PF-8380.

Assay	**IC_{50}** (nM ± SD)
Human Enzyme FS-3	2.8 ± 0.16 (n=4)
Human Enzyme LPC	1.7 ± 0.6 (n=3)
Murine Enzyme FS-3	1.16 ± 0.07 (n=3)
Fetal Fibroblast Cell LPC	1.15 ± 0.18 (n=3)
Human Whole Blood	101 ± 0.036 (n=3)

Downloaded from jpet.aspetjournals.org at ASPET Journals on April 18, 2024

JPET Fast Forward. Published on April 14, 2010 as DOI: 10.1124/jpet.110.165845
This article has not been copyedited and formatted. The final version may differ from this version.

Table 2. Pharmacokinetics of PF-8380 in rat

Parameter	**Units**	**IV 1mg/kg (n=2)**	**Oral 1 mg/kg (n=5)**	**Oral 3 mg/kg (n=3)**	**Oral 10 mg/kg (n=3)**	**Oral 30 mg/kg (n=3)**	**Oral 100 mg/kg (n=3)**
Dose	mg/kg	1	1	3	10	30	100
AUC	µM*Hours	1.12	0.480 ± 0.120	2.25 ± 0.54	9.22 ± 2.75	20.6 ± 6.2	56.6 ± 11.0
Clearance	mL/min/kg	31					
Vdss	L/kg	3.2					
Cmax	µM		0.124 ± 0.025	0.922 ± 0.120	2.55 ± 0.75	4.23 ± 0.50	6.19 ± 1.06
Tmax	Hours		0.60 ± 0.22	0.50 ± 0.0	0.67 ± 0.29	0.42 ± 0.14	3.3 ± 1.2
Effective t1/2	Hours	1.2					
Terminal t1/2	Hours	1.7	2.1 ± 0.7	1.5 ± 0.2	2.2 ± 0.5	2.8 ± 0.3	4.3 ± 1.2
Bioavailability	%		43 ± 9	68 ± 16	83 ± 25	62 ± 19	52 ± 10

Downloaded from jpet.aspetjournals.org at ASPET Journals on April 18, 2024

JPET Fast Forward. Published on April 14, 2010 as DOI: 10.1124/jpet.110.165845
This article has not been copyedited and formatted. The final version may differ from this version.

Table 3. Inhibitory E_{max} Model Parameters

	C16:0 (95% CI)	C18:0 (95% CI)	C20:0 (95% CI)
EC_{50} [nmol/L]	54.7 (31.1 – 78.3)	84.6 (19.7 – 149)	51.7 (29.1 – 74.3)
E_{max} [ng/mL]	19.6 (18.4 – 20.8)	15.9 (14.2 – 17.6)	276.7 (259.4 – 293.9)
E_0 [ng/mL]	3.25 (2.30 – 4.21)	3.10 (1.64 – 4.56)	48.3 (34.8 – 61.7)

Downloaded from jpet.aspetjournals.org at ASPET Journals on April 18, 2024

JPET Fast Forward. Published on April 14, 2010 as DOI: 10.1124/jpet.110.165845
This article has not been copyedited and formatted. The final version may differ from this version.

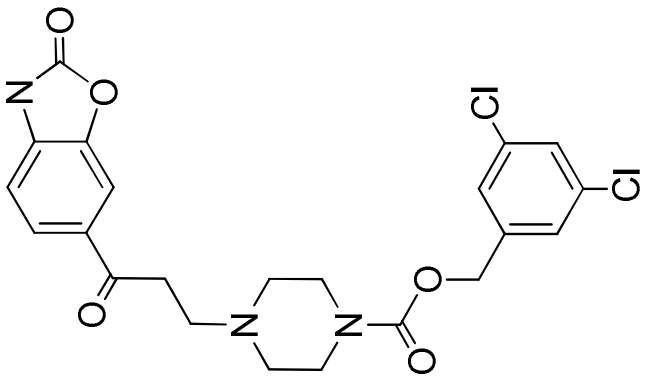

Figure 1

Downloaded from jpet.aspetjournals.org at ASPET Journals on April 18, 2024

Figure 2

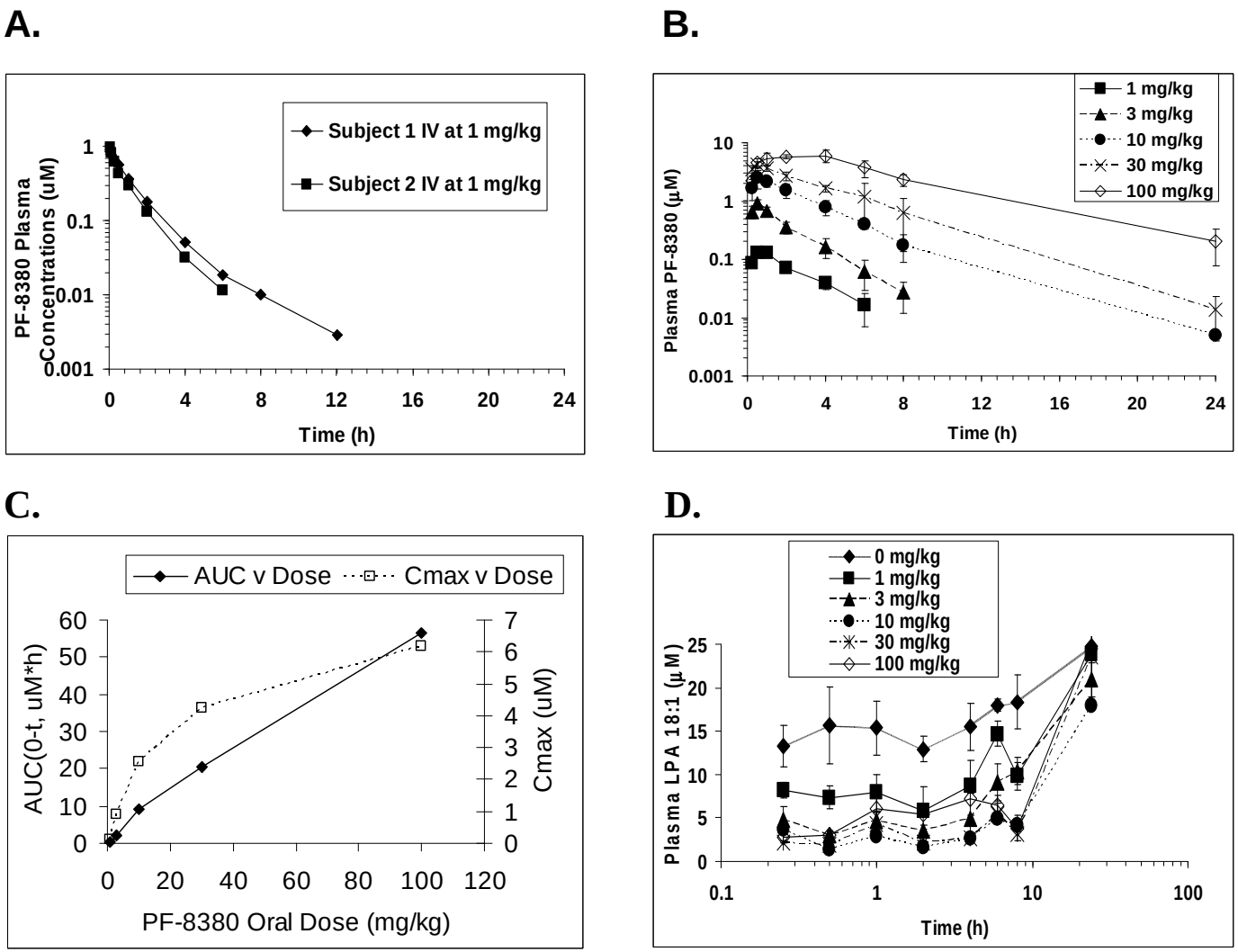

JPET Fast Forward. Published on April 14, 2010 as DOI: 10.1124/jpet.110.165845
This article has not been copyedited and formatted. The final version may differ from this version.

Downloaded from jpet.aspetjournals.org at ASPET Journals on April 18, 2024

Figure 3

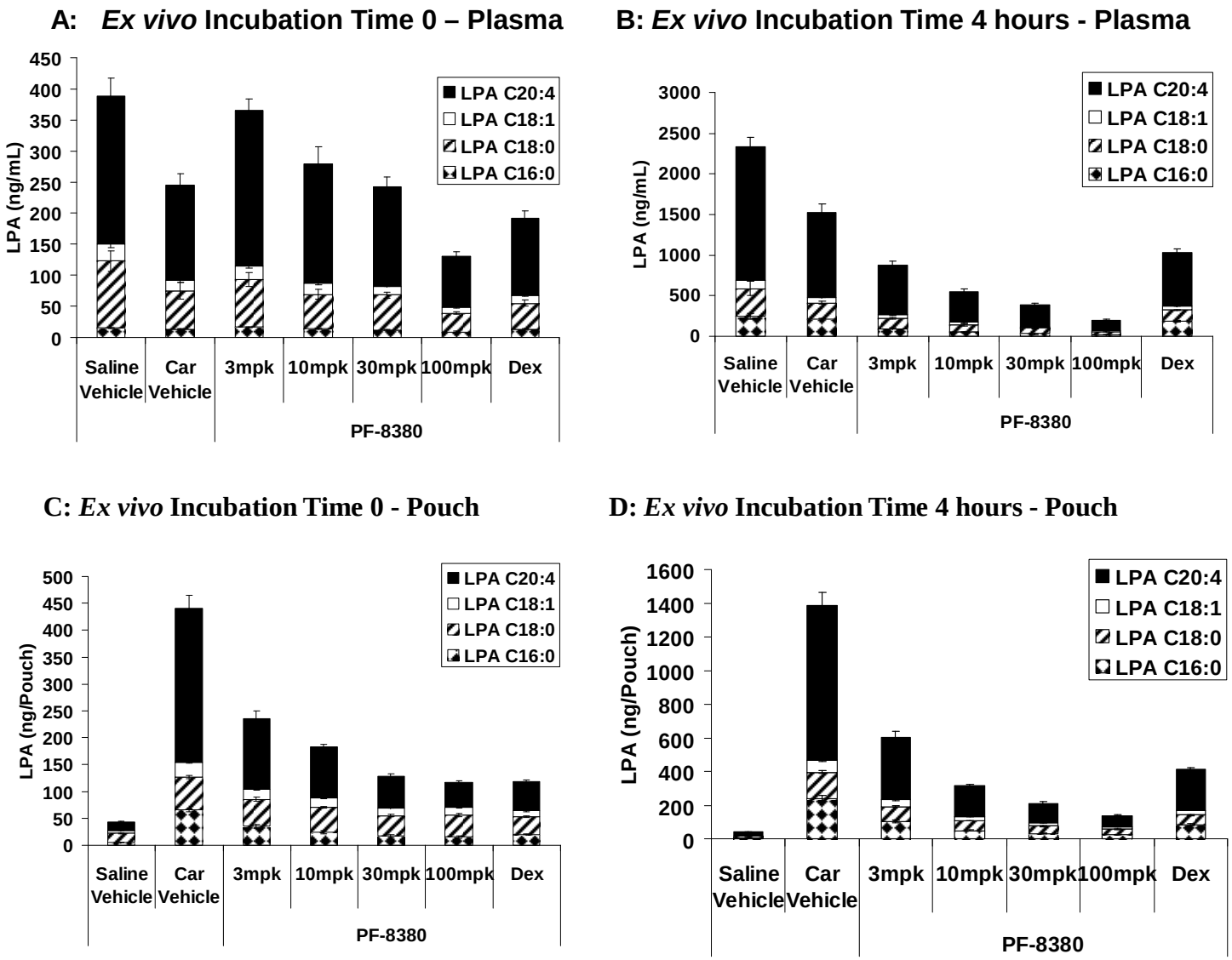

JPET Fast Forward. Published on April 14, 2010 as DOI: 10.1124/jpet.110.165845
This article has not been copyedited and formatted. The final version may differ from this version.

Downloaded from jpet.aspetjournals.org at ASPET Journals on April 18, 2024

Figure 4

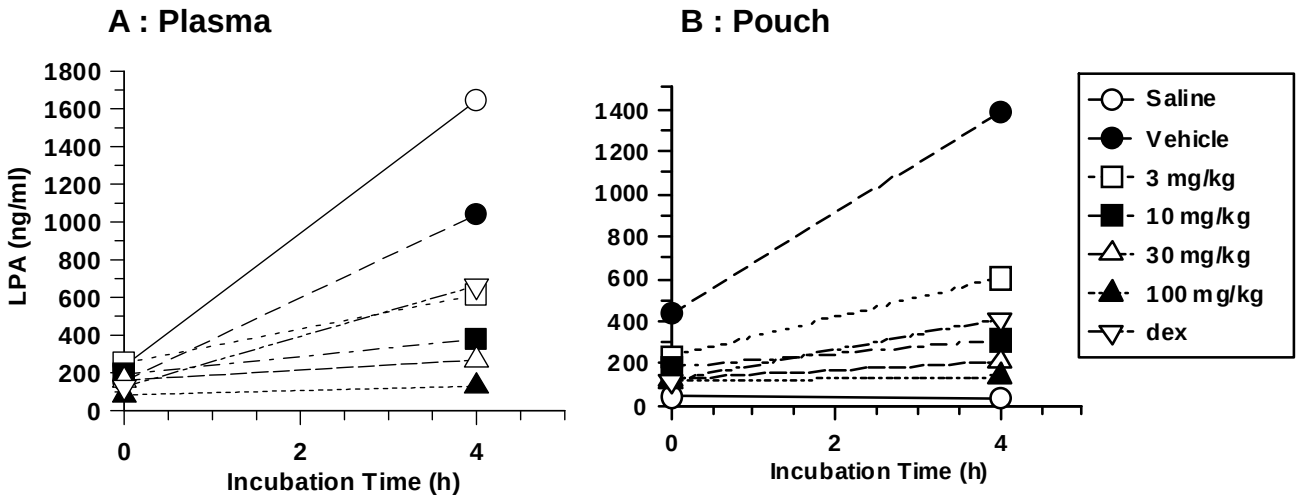

JPET Fast Forward. Published on April 14, 2010 as DOI: 10.1124/jpet.110.165845
This article has not been copyedited and formatted. The final version may differ from this version.

Downloaded from jpet.aspetjournals.org at ASPET Journals on April 18, 2024

Figure 5

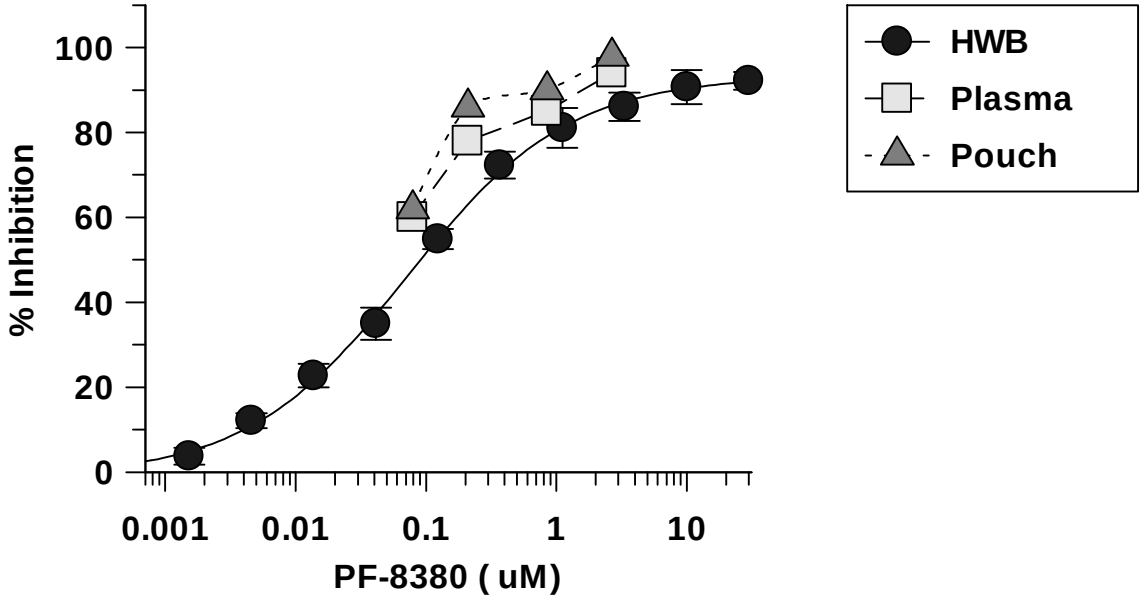

JPET Fast Forward. Published on April 14, 2010 as DOI: 10.1124/jpet.110.165845
This article has not been copyedited and formatted. The final version may differ from this version.

Downloaded from jpet.aspetjournals.org at ASPET Journals on April 18, 2024

Figure 6

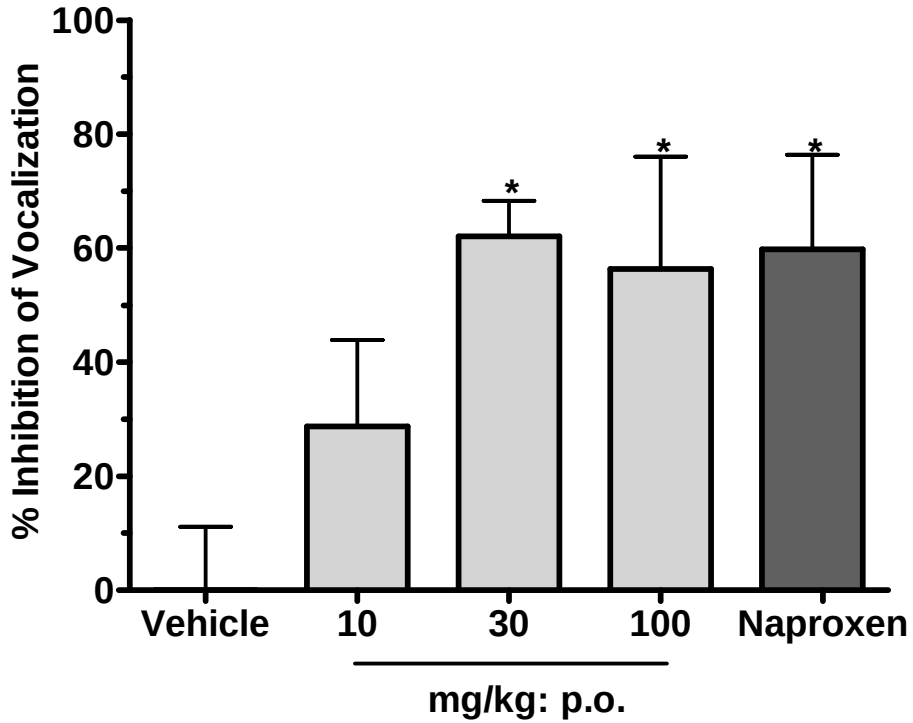

JPET Fast Forward. Published on April 14, 2010 as DOI: 10.1124/jpet.110.165845
This article has not been copyedited and formatted. The final version may differ from this version.

Downloaded from jpet.aspetjournals.org at ASPET Journals on April 18, 2024